ChemPubSoc Europe

DOI: 10.1002/chem.201701067

CHEMISTRY
A European Journal
Communication

Halogen Bonding

Designer Metallic Acceptor-Containing Halogen Bonds: General Strategies

Xinxing Zhang* and Kit Bowen*[a]

Abstract: Being electrostatic interactions in nature, hydrogen bonding (HB) and halogen bonding (XB) are considered to be two parallel worlds. In principle, all the applications that HB have could also be applied to XB. However, there has been no report on an anionic, metallic XB acceptor, but metal anions have been observed to be good HB acceptors. This missing mosaic piece of XB theory is because common metal anions are reactive for XB donors. In view of this, two strategies are proposed for designing metallic acceptor-containing XB using ab initio calculations. The first one is to utilize a metal cluster anion with a high electron detachment energy, such as the superatom, Al_{13}^- as the XB acceptor. The second strategy is to design a ligand-passivated/protected metal core that can maintain the negative charge; several exotic clusters, such as PtH_5^-, $PtZnH_5^-$, and $PtMgH_5^-$, are used as examples. Based on these two strategies, it is anticipated that more metallic acceptor-containing XBs will be discovered.

Halogen bonding (XB), a type of non-covalent interaction, has become an emerging field both experimentally[1] and theoretically[2] in recent years. The nature of halogen bonding is electrostatic: covalently bonded, polarizable halogen atoms have positive electrostatic potential regions on the opposite end of the covalent bond, and the equatorial side is negative.[3,4] The attractions between the positive region and nucleophiles, and between the negative equatorial site and electrophiles are the halogen bonding. The positive region was first named as the "σ-hole" in 2007[5] because it is induced by the σ-bond between the halogen atom and the atom bonded to it. The size of the σ-hole increases with increasing polarizability of the halogen atoms, that is, I > Br > Cl > F, but can also be tuned by other electron-donating or -withdrawing functional groups in the molecule.[6,7] Since the nature of XB was resolved, it has been widely applied into many fields such as supramolecular chemistry and crystal engineering in which XB is the driving force of self-assembly.[8–11] The existence of XB in biological systems was also recognized.[7,12] Several experiments have studied XB spectroscopically in the gas phase.[13–15]

Hydrogen bonding (HB), on the other hand, has a much longer history and is more extensively studied compared to XB. HB and XB are the same in nature, both being non-covalent, weak, electrostatic interactions featuring electron density donation from a rich to a poor site. Hence, XB is viewed as "a world parallel to HB",[16,17] for example, HB is also utilized as the driving force of crystal engineering.[18] In view of this, one would anticipate that any place that HB can play a role XB could do the same, and they already do on copious fronts. However, the missing mosaic piece of XB compared to HB is the interaction between an XB donor and a negatively charged metal acceptor. As shown in Figure 1 A, a water molecule can form an HB with a gold anion. By forming the HB, the metal anion is stabilized. Water-solvated metal anions have been observed in systems such as Cu^-, Ag^-, Au^-, and Cs^-.[19–22] Similar HB was also observed in Au^- complexes.[23] In principle, a σ-hole of a organohalogen could also form an XB with a metal anion, however, there have been no studies of such. The absence is because atomic metal anions are too reactive towards organohalogens. In Figure 1 B, using triflurobromomethane (CF_3Br) as an example XB donor, our calculations show that instead of forming a weak interaction between Br and the gold anion, the system prefers to react to form a Au–Br coordination bond while lengthening the C–Br bond to 2.13 Å (1.95 Å in free CF_3Br). The Au–Br bond length, 2.69 Å, is significantly shorter than a typical halogen bond (ca. 3.0 Å), [2] showing that it is not an XB. The gold anion could also insert into the C–Br bond to form the structure 1 C, the energy of which is 2.38 eV lower than that of 1 B. Such a huge gain in energy makes 1 C more thermodynamically favored than 1 B. It is also worth pointing out that the structure of 1 C is similar to that of a Grignard reagent because both Mg and Au^- have two valence electrons.[24] Here we chose Au^- because the electron affinity (EA) of the Au atom is the highest of all metal atoms (2.31 eV).[25] If the inert Au^- cannot form XB, other metal anions are even more unlikely to do so. Given the above dis-

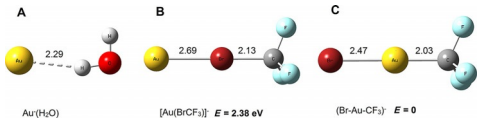

Figure 1. Calculated structures of A) $Au^-(H_2O)$, B) $[Au(BrCF_3)]^-$ and C) $[Br\text{-}Au\text{-}CF_3]^-$. Bond lengths are in Å and relative energies are in eV.

[a] Dr. X. Zhang, Prof. K. Bowen
Departments of Chemistry and Material Sciences
Johns Hopkins University
Baltimore, Maryland, MD 21218 (USA)
E-mail: xzhang54@jhu.edu
kbowen@jhu.edu

Supporting information for this article can be found under: http://dx.doi.org/10.1002/chem.201701067.

cussions, one needs to have a system that is stable enough to prevent reactions between the XB donor and acceptor. Two strategies are proposed here: the negatively charged metal side has to be 1, highly stable (with high EA) or 2, be protected/passivated by other ligands while allowing the metal center to maintain the negative charge.

The theoretical methods used in the current study are provided in the Supporting Information. All the results in the following sections are from DFT-based calculations using the PBEPBE functional. The results using the M06-2x functional are presented in the Supporting Information. The two functionals have been reported to be reliable methods[26] for XB calculations. Even though the goal of the current study is not to compare the advantages and disadvantages of different methods applied to XB, the two methods used here obtained satisfactory consistency. The CF_3Br molecule is used as the example XB donor in the whole study.

We first discuss the plausibility of strategy 1. The bottom line of constructing an XB between a metal anion and organohalogen is that the metal anion should be capable of holding the negative charge, otherwise it will be oxidized by the halogen atom like the scenario in Figure 1. Hence, the metal side should have high EA, which would better be close to, or even higher than the EA of a halogen. So the Al_{13} cluster should be a good candidate. With an EA of 3.57 eV, which is very close to Br, Al_{13} is considered to be the superatom of Br.[27] The corresponding anion Al_{13}^- is highly stable, and can form salts like KAl_{13}, which is similar to KBr.[28] Al_{13}^- is inert even towards the reaction with O_2.[29] Therefore, the XB in the $CF_3Br{-}Al_{13}^-$ complex should be stable and similar to that of $CF_3Br{-}Br^-$. Figure 2A presents the structures of $CF_3Br{-}Al_{13}^-$ and $CF_3Br{-}Br^-$. For $CF_3Br{-}Al_{13}^-$, the Al_{13}^- moiety possesses an icosahedral structure. The C–Br bond is perpendicular to one of the 20 triangular faces of the icosahedron. The distance from the Br atom to the center of the equilateral triangle is 3.38 Å, indicating that the interaction between CF_3Br and Al_{13}^- is a weak, long-distance, non-covalent bond. By replacing Al_{13}^- with Br^-, we have the structure of $CF_3Br{-}Br^-$. The XB length is 2.94 Å in this case, shorter than that of $CF_3Br{-}Al_{13}^-$. This is because the negative charge is distributed in the whole big cluster, Al_{13}^-, therefore, only part of the negative charge is effective in forming the XB, but in Br^-, the negative charge is more concentrated. The XB strength is calculated using the formula $D_0[CF_3Br{-}Y^-] = E[CF_3Br] + E[Y^-] - E[CF_3Br{-}Y^-]$ (Table 1), where Y^- denotes the XB acceptor. Zero-point energy is corrected in these calculations. $D_0[CF_3Br{-}Al_{13}^-]$ (0.22 eV) is weaker than $D_0[CF_3Br{-}Br^-]$ (0.70 eV), in consistency with the XB lengths. The 0.22 eV for $CF_3Br{-}Al_{13}^-$, even though relatively weaker, is still significant, and it is almost the same as the HB strength of a water dimer,[30] making it possible to be observed in future experiments.

Table 1. The XB bond strength $D_0[CF_3Br{-}Y^-]$ of different systems calculated from the PBEPBE functional. All values are in eV.

Species[a]	X–Br$^-$	X–Al_{13}^-	X–PtH_5^-	X$_2$–PtH_5^-	X–$PtMgH_5^-$	X–$PtZnH_5^-$
D_0	0.70	0.22	0.56	0.47	0.48	0.51

[a] CF_3Br is denoted as X for short.

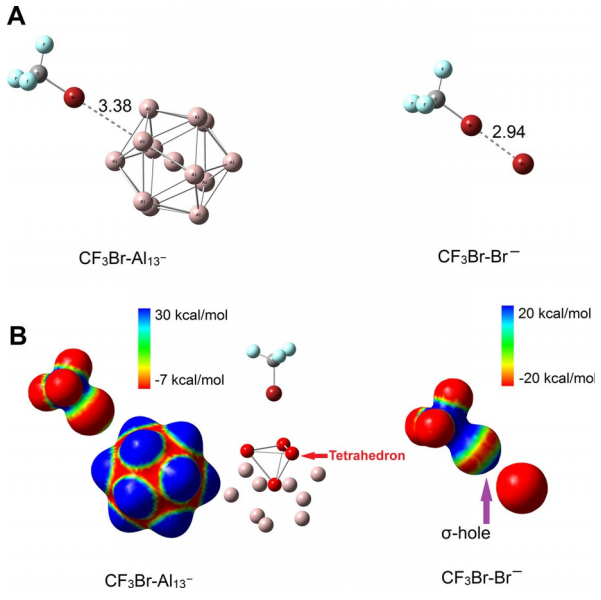

Figure 2. A) Structures of $CF_3Br{-}Al_{13}^-$ and $CF_3Br{-}Br^-$. B) Electrostatic potential (ESP) surfaces of $CF_3Br{-}Al_{13}^-$ and $CF_3Br{-}Br^-$. The induced positive (blue), negative (red) potentials are mapped on the 0.02 *e*/bohr^3 surface for $CF_3Br{-}Al_{13}^-$ and 0.04 *e*/bohr^3 surface for $CF_3Br{-}Br^-$. Different potential ranges are given to obtain best visual effect.

In order to better visualize the halogen bonding, Figure 2B presents the electrostatic potential (ESP) of $CF_3Br{-}Al_{13}^-$ and $CF_3Br{-}Br^-$. The induced positive (blue) and negative (red) electrostatic potentials are mapped on the 0.02 or 0.04 *e*/bohr^3 surfaces. For $CF_3Br{-}Al_{13}^-$, The positive end of Br (the σ-hole, blue) points to the Al_{13}^- moiety's negative charge (red), which is located at the center of each tetrahedron and is composed of the three Al atoms on each triangular face and the center Al atom (highlighted in Figure 2B). Each red site of Al_{13}^- is essentially a 4-center-2-electron bond. There are 20 tetrahedrons in total, making the skeletal electrons to be 40, which is equal to the total number of valence electrons of 13 Al atoms plus the negative charge.[27] Therefore, the Br atom points towards the face other than the vertex or edge of the icosahedron. For $CF_3Br{-}Br^-$, the XB between the σ-hole (blue) and Br^- (red) is obvious.

We next discuss the second strategy of designing metal-containing XB by protecting/passivating the metal core with ligands. Typical ligands in metal complexes such as chlorine are often oxidative, making the metal center positively charged, for example, Fe^{3+} in $[FeCl_6]^{3-}$. For other metal complexes like $[Ti(CO)_6]^{2-}$ and $[V(CO)_6]^-$,[31,32] even though the metal cores are negatively charged, they are fully surrounded by the ligands, making it impossible for a XB donor to access the metal. In view of this, two criteria are needed for the second strategy: the metal should be 1) negatively charged and 2) have at least one open site to accept the XB. Several exotic cluster anions, PtH_5^-, $PtMgH_5^-$, and $PtZnH_5^-$ drew our attention. They have been synthesized in the gas phase and characterized by anion

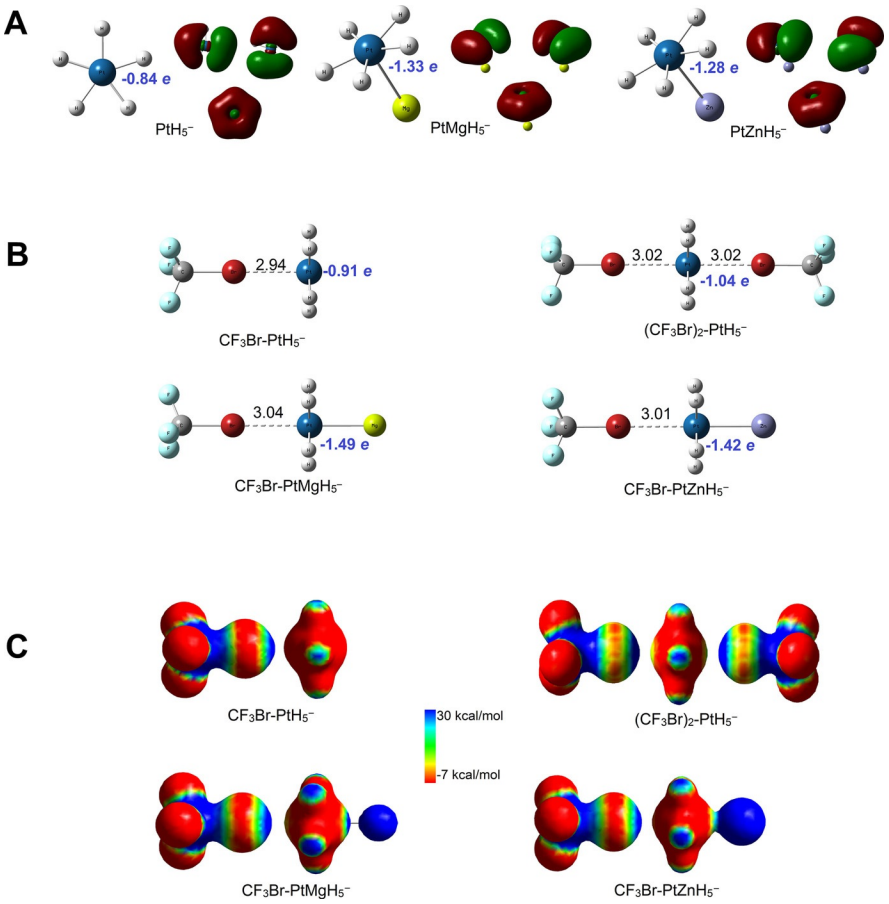

Figure 3. A) Structures and σ-aromatic MOs of PtH_5^-, $PtMgH_5^-$, and $PtZnH_5^-$. The charges on Pt atoms are marked in blue. B) Structures of $(CF_3Br)_{1,2}$–PtH_5^-, CF_3Br–$PtMgH_5^-$, and CF_3Br–$PtZnH_5^-$. The charges on Pt atoms are marked in blue. C) Electrostatic potential (ESP) surfaces of $(CF_3Br)_{1,2}$–PtH_5^-, CF_3Br–$PtMgH_5^-$, and CF_3Br–$PtZnH_5^-$. The induced positive (blue), negative (red) potentials are mapped on the 0.04 *e*/bohr^3 surfaces.

photoelectron spectroscopy.[33–35] In these clusters, the five H atoms form a ring and coordinate with the center Pt atom, and the Mg or Zn atom approaches the Pt center perpendicularly to the PtH_5 plane. Thus, PtH_5^- has a D_{5h} symmetry; $PtMgH_5^-$ and $PtZnH_5^-$ have C_{5v} symmetries (Figure 3 A). More importantly, the H_5^- ring, stabilized by the center Pt atom, has six electrons in total, resulting in a unique stabilization effect called the σ-aromaticity by fulfilling the Hückel's $4n+2$ rule. The σ-aromaticity makes these clusters unusually stable; their intensities in the mass spectra are extremely intense, hence they are named as the "magic numbers".[33–35] In Figure 3 A, we present the three occupied and highly delocalized σ-aromatic molecular orbitals (MOs) of the clusters. Besides, since the electronegativity of Pt is higher than those of H, Mg, or Zn, the Pt centers of these clusters are negatively charged by −0.84 *e*, −1.33 *e*, −1.28 *e* for PtH_5^-, $PtMgH_5^-$, and $PtZnH_5^-$, respectively, which is the key that makes the XB possible. Due to the geometries, PtH_5^- has two open sites, $PtMgH_5^-$ and $PtZnH_5^-$ have one open site to accept one or two XB donors. Therefore, PtH_5^-, $PtMgH_5^-$, and $PtZnH_5^-$ fulfill the above two criteria of the second strategy.

Figure 3 B presents the structures of $(CF_3Br)_{1,2}$-PtH_5^-, CF_3Br-$PtMgH_5^-$, and CF_3Br-$PtZnH_5^-$. In these clusters, the XB acceptors, that is, the Pt-containing sides maintain their structures in Figure 3 A, and the XB bond lengths are all in the proximity of 3 Å, indicating that they are indeed XBs. Similar to that of CF_3Br-Al_{13}^-, the C–Br bond in these clusters are all perpendicular to the PtH_5 plane and pointing towards the Pt atoms where the negative charges dwell. The XB strengths, D_0, of all of these four systems are tabulated in Table 1. All of them are around 0.5 eV. These numbers are higher than a lot of HB energies.[17] Furthermore, the trend of D_0 is in consistency of the XB lengths. For example, $D_0[CF_3Br$–$PtH_5^-]$ is higher than $D_0[(CF_3Br)_2$–$PtH_5^-]$, so the XB length in CF_3Br–PtH_5^- is shorter than in $(CF_3Br)_2$–PtH_5^-. Same trend can be found in CF_3Br–$PtMgH_5^-$ and CF_3Br–$PtZnH_5^-$. In Figure 3 B, we also marked the negative charges on each Pt atoms (*e*) obtained from natural population analysis (NPA) to compare with those in Figure 3 A. Upon forming the XB, the negative charges on the Pt atoms increased. This is because the XB induces the Pt atoms to draw more charges from the adjacent H, Mg, and Zn. Figure 3 C exhibits the ESP of $(CF_3Br)_{1,2}$–PtH_5^-, CF_3Br–$PtMgH_5^-$, and CF_3Br–$PtZnH_5^-$. The induced electrostatic potentials are all mapped on the 0.04 *e*/bohr^3 surfaces. Again, the positive end of Br (blue), that is, the σ-hole, is pointing towards the negative Pt atom (red) in all of these four cases. For the second strategy, the XB acceptors do not necessarily need to have very high EA.

In summary, we have proposed two strategies for designing metal-containing XB and provided several examples for each. Since negatively charged metals are usually reactive towards organohalogens, the metallic XB acceptor has to be carefully designed in order to maintain the integrity of both of the XB donor and acceptor. The first strategy is straightforward; we choose high-EA metal cluster that can be inert when they encounter an XB donor. Al_{13}^-, the superatom of Br^-, is used as an example. The second strategy is trickier. Other than using bare metals, one could also protect/passivate the metal cores. Efforts are needed to design stable metal complexes where the metal core is negatively charged in the presence of ligands and has at least one open site for the XB donor. Three clusters that meet these criteria, PtH_5^-, $PtMgH_5^-$, and $PtZnH_5^-$, are used to test the second strategy. Based on these two strategies, we anticipate that this work can be a kick-start for more experimental and theoretical efforts to design metal-containing XBs, so that the XB world can be genuinely parallel to the HB world.

Acknowledgements

This material is based upon work supported by the (U.S.) National Science Foundation under Grant No. CHE-1360692 and CHE-1664182.

Conflict of interest

The authors declare no conflict of interest.

Keywords: aluminium · bond theory · halogen bonding · metal hydrides · superatoms

[1] G. Cavallo, P. Metrangolo, R. Milani, T. Pilati, A. Priimagi, G. Resnati, G. Terraneo, *Chem. Rev.* **2016**, *116*, 2478 – 2601.
[2] M. H. Kolář, P. Hobza, *Chem. Rev.* **2016**, *116*, 5155 – 5187.
[3] T. Brinck, J. S. Murray, P. Politzer, *Int. J. Quantum Chem.* **1992**, *44*, 57 – 64.
[4] T. Brinck, J. S. Murray, P. Politzer, *Int. J. Quantum Chem.* **1993**, *48*, 73 – 88.
[5] T. Clark, M. Hennemann, J. S. Murray, P. Politzer, *J. Mol. Model.* **2007**, *13*, 291 – 296.
[6] P. Politzer, P. Lane, M. C. Concha, Y. Ma, J. S. Murray, *J. Mol. Model.* **2007**, *13*, 305 – 311.
[7] P. Auffinger, F. A. Hays, E. Westhof, P. S. Ho, *Proc. Natl. Acad. Sci. USA* **2004**, *101*, 16789 – 16794.
[8] E. Corradi, S. V. Meille, M. T. Messina, P. Metrangolo, G. Resnati, *Angew. Chem.* **2000**, *112*, 1852 – 1856.
[9] P. Metrangolo, F. Meyer, T. Pilati, G. Resnati, G. Terraneo, *Angew. Chem. Int. Ed.* **2008**, *47*, 6114 – 6127; *Angew. Chem.* **2008**, *120*, 6206 – 6220.
[10] L. Meazza, J. A. Foster, K. Fucke, P. Metrangolo, G. Resnati, Jonathan W. Steed, *Nat. Chem.* **2013**, *5*, 42 – 47.
[11] V. Amico, S. V. Meille, E. Corradi, M. T. Messina, G. Resnati, *J. Am. Chem. Soc.* **1998**, *120*, 8261 – 8262.
[12] L. A. Hardegger, B. Kuhn, B. Spinnler, L. Anselm, R. Ecabert, M. Stihle, B. Gsell, R. Thoma, J. Diez, J. Benz, J.-M. Plancher, G. Hartmann, D. W. Banner, W. Haap, F. Diederich, *Angew. Chem. Int. Ed.* **2011**, *50*, 314 – 318; *Angew. Chem.* **2011**, *123*, 329 – 334.
[13] S. L. Stephens, N. R. Walker, A. C. Legon, *J. Chem. Phys.* **2011**, *135*, 224309.
[14] H. I. Bloemink, J. H. Holloway, A. C. Legon, *Chem. Phys. Lett.* **1996**, *254*, 59 – 68.
[15] C. Domene, P. W. Fowler, A. C. Legon, *Chem. Phys. Lett.* **1999**, *309*, 463 – 470.
[16] P. Metrangolo, H. Neukirch, T. Pilati, G. Resnati, *Acc. Chem. Res.* **2005**, *38*, 386 – 395.
[17] Z. P. Shields, J. S. Murray, P. Politzer, *Int. J. Quantum Chem.* **2010**, *110*, 2823 – 2832.
[18] J. Bernstein, R. E. Davis, L. Shimoni, N.-L. Chang, *Angew. Chem. Int. Ed. Engl.* **1995**, *34*, 1555 – 1573; *Angew. Chem.* **1995**, *107*, 1689 – 1708.
[19] W. Zheng, X. Li, S. Eustis, A. Grubisic, O. Thomas, H. deClercq, K. Bowen, *Chem. Phys. Lett.* **2007**, *444*, 232 – 236.
[20] C. Chi, H. Xie, Y. Li, R. Cong, M. Zhou, Z. Tang, *J. Phys. Chem. A* **2011**, *115*, 5380 – 5386.
[21] G. J. Rathbone, T. Sanford, D. Andrews, W. Carl Lineberger, *Chem. Phys. Lett.* **2005**, *401*, 570 – 574.
[22] Z. Zeng, C. Liu, G. Hou, G. Feng, H. Xu, Y. Gao, W. Zheng, *J. Phys. Chem. A* **2015**, *119*, 2845 – 2856.
[23] H. Nuss, M. Jansen, *Angew. Chem. Int. Ed.* **2006**, *45*, 4369 – 4371; *Angew. Chem.* **2006**, *118*, 4476 – 4479.
[24] D. A. Shirley, *Org. React; The Synthesis of Ketones from Acid Halides and Organometallic Compounds of Magnesium, Zinc, and Cadmium*, Wiley, **1954**, *8*, 28 – 58.
[25] X. Zhang, E. Lim, S. K. Kim, K. H. Bowen, *J. Chem. Phys.* **2015**, *143*, 174305.
[26] S. Kozuch, J. M. L. Martin, *J. Chem. Theory Comput.* **2013**, *9*, 1918 – 1931.
[27] a) D. E. Bergeron, A. W. Castleman, T. Morisato, S. N. Khanna, *Science* **2004**, *304*, 84 – 87; b) X. Li, L.-S. Wang, *Phys. Rev. B* **2002**, *65*, 153404.
[28] W.-J. Zheng, O. C. Thomas, T. P. Lippa, S.-J. Xu, K. H. Bowen, *J. Chem. Phys.* **2006**, *124*, 144304.
[29] R. E. Leuchtner, A. C. Harms, A. W. Castleman, Jr., *J. Chem. Phys.* **1989**, *91*, 2753 – 2754.
[30] C. Leforestier, K. Szalewicz, A. van der Avoird, *J. Chem. Phys.* **2012**, *137*, 014305.
[31] K. G. Caulton, R. F. Fenske, *Inorg. Chem.* **1968**, *7*, 1273 – 1284.
[32] K. M. Chi, S. R. Frerichs, S. B. Philson, J. E. Ellis, *J. Am. Chem. Soc.* **1988**, *110*, 303 – 304.
[33] X. Zhang, G. Liu, K.-H. Meiwes-Broer, G. Ganteför, K. H. Bowen, *Angew. Chem. Int. Ed.* **2016**, *55*, 9644 – 9647; *Angew. Chem.* **2016**, *128*, 9796 – 9799.
[34] X. Zhang, G. Liu, G. Gantefoer, K. H. Bowen, A. N. Alexandrova, *J. Phys. Chem. Lett.* **2014**, *5*, 1596 – 1601.
[35] X. Zhang, G. Gantefoer, A. Alexandrova, K. H. Bowen, *Phys. Chem. Chem. Phys.* **2016**, *18*, 19345 – 19349.

Manuscript received: March 9, 2017
Accepted Article published: March 13, 2017
Final Article published: March 29, 2017